

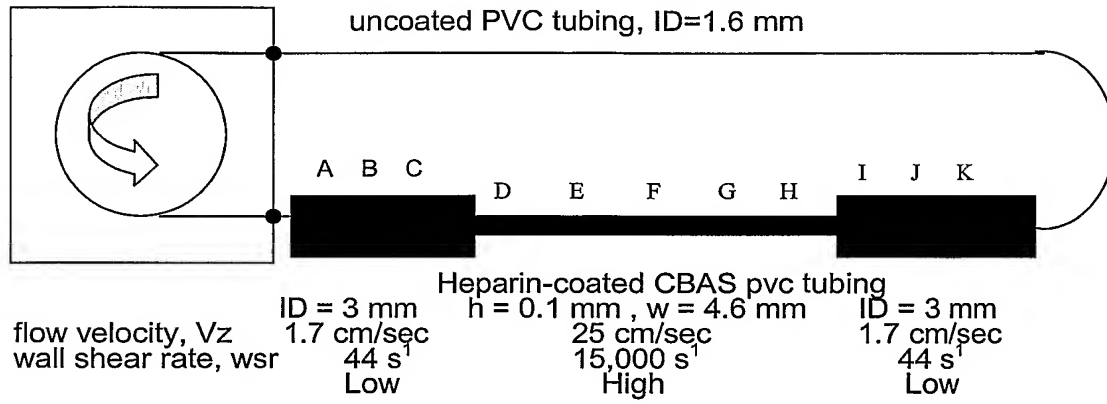
FIG. 1**IN VITRO FLOW MODEL**

FIG. 2

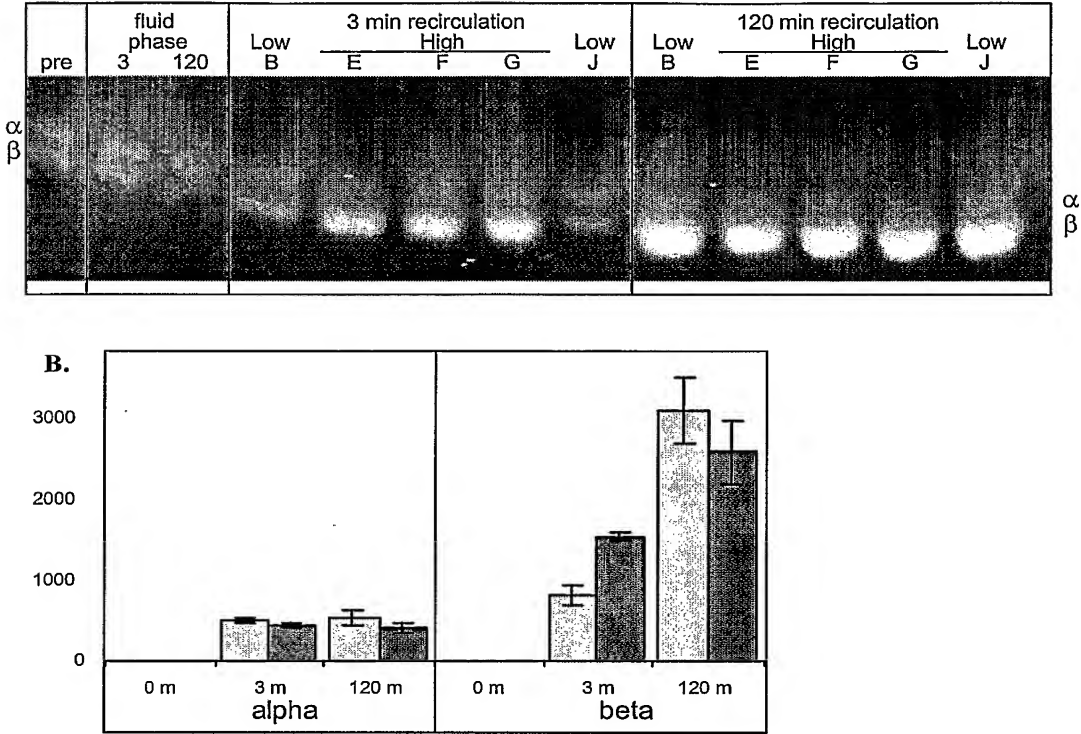
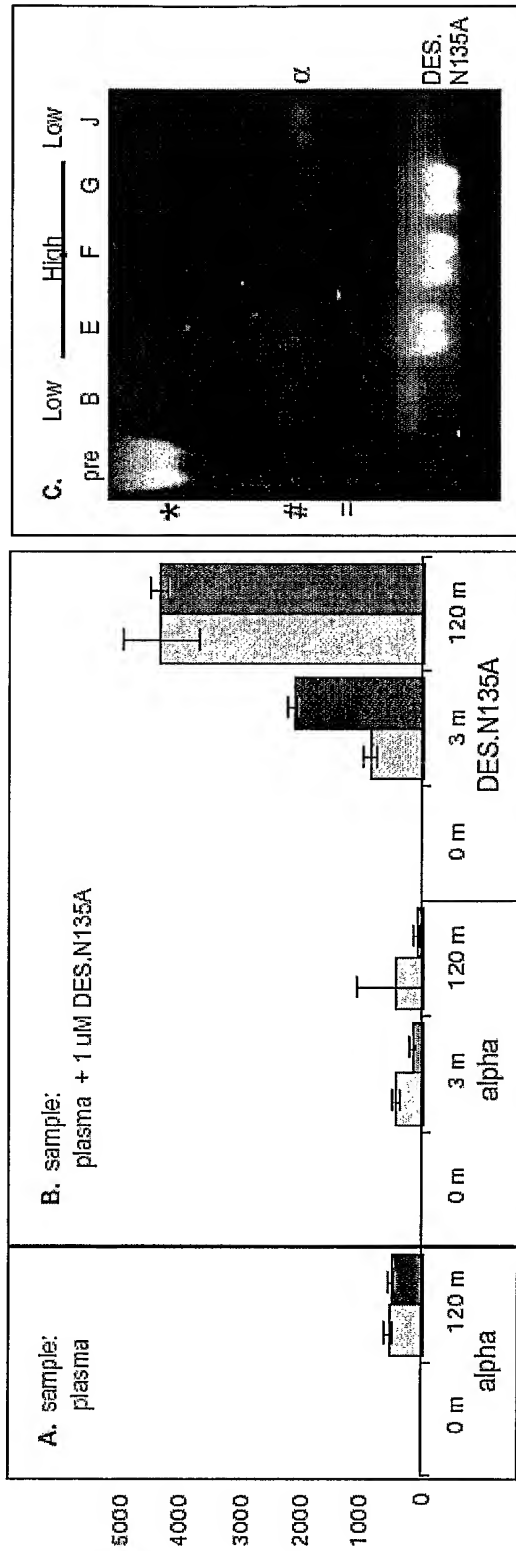


FIG. 3



SDS-PAGE of ATIII loaded onto heparin-coated tubing during 3m recirculation. "pre" is the pre-circulation sample containing diluted plasma (50%) plus 1 uM DES.N135A. Low and high flow segments are marked as in Fig. 1.

Surface-bound ATIII (ng / segment; avg \pm SD) for heparin-coated tubing exposed to plasma \pm DES.N135A ATII under low (light gray) and high (dark gray) flow velocity conditions.

FIG. 4

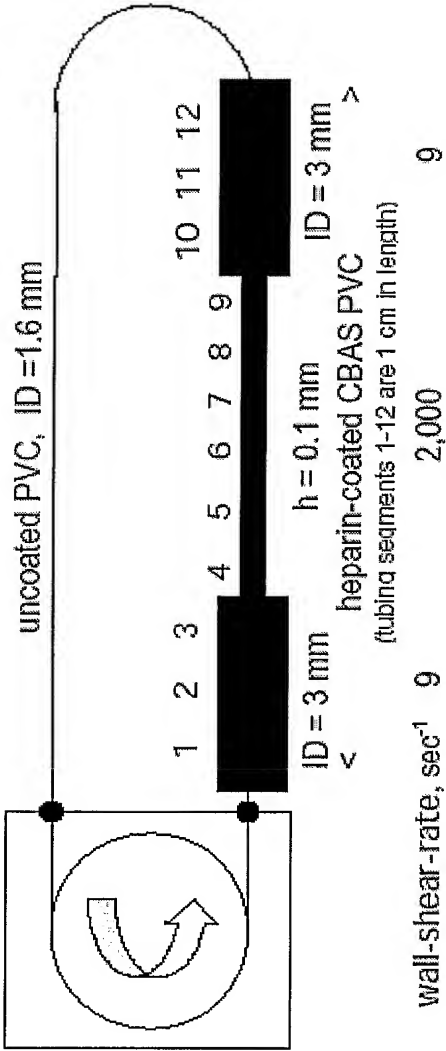


FIG. 5

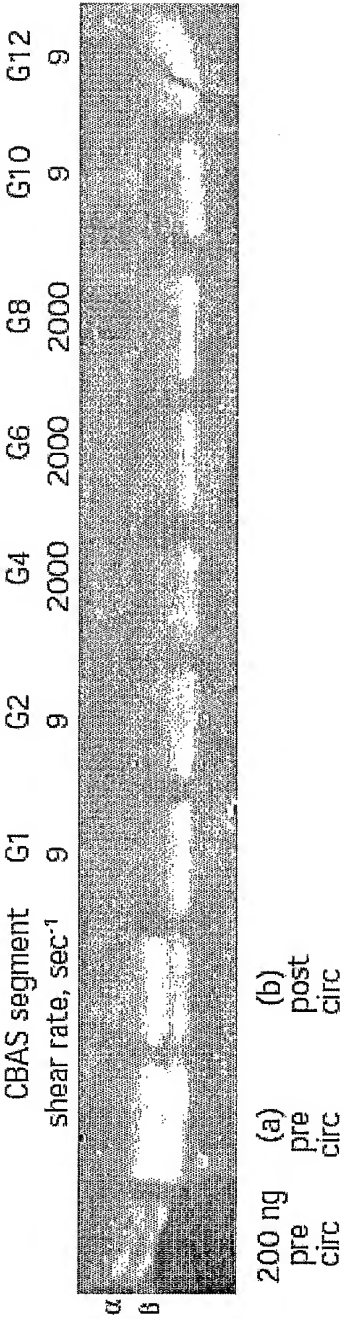


FIG. 6

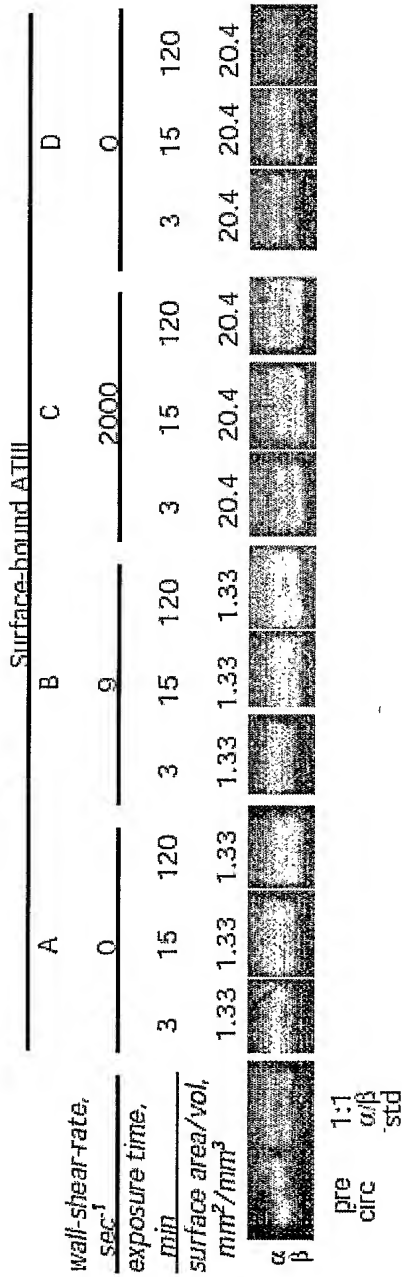


FIG. 7

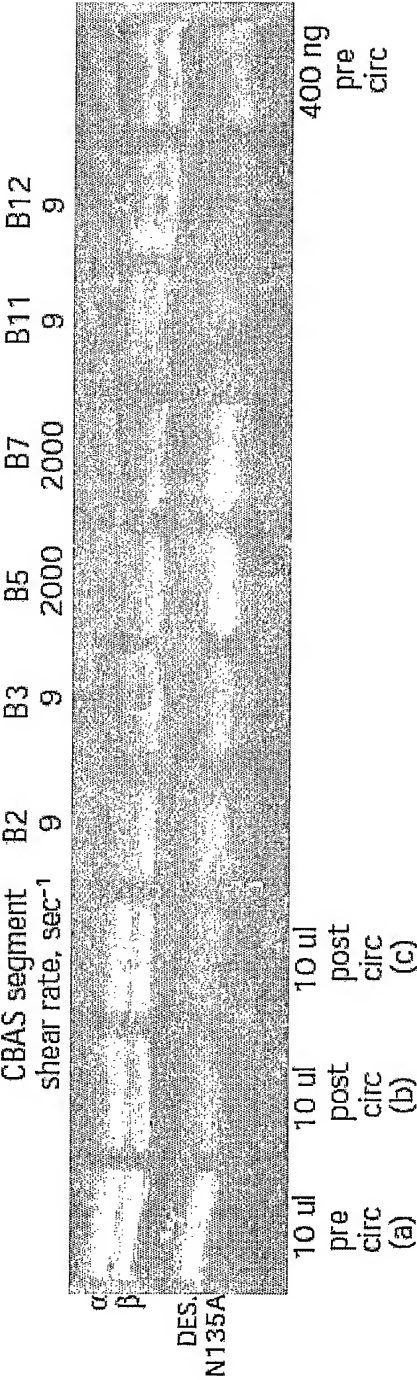


FIG. 8

IN VITRO FLOW MODEL

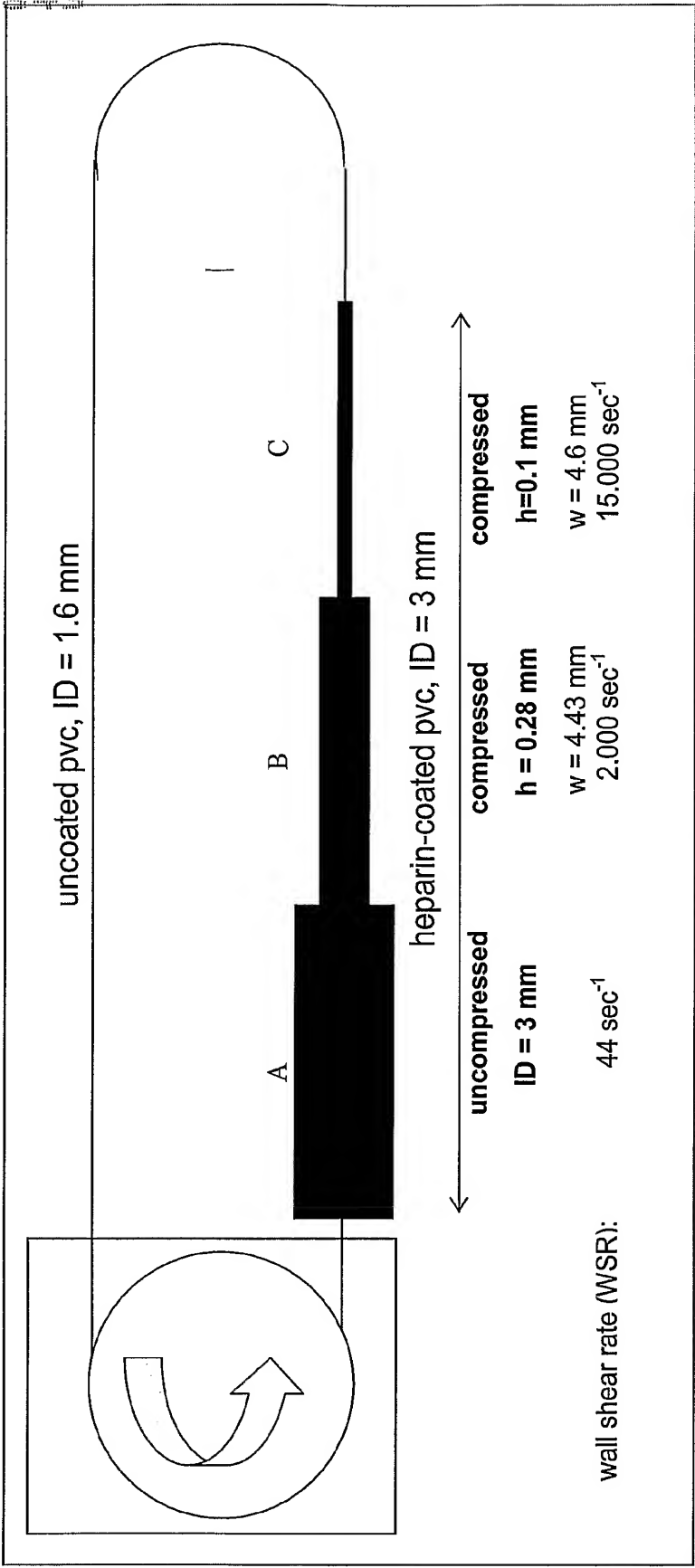
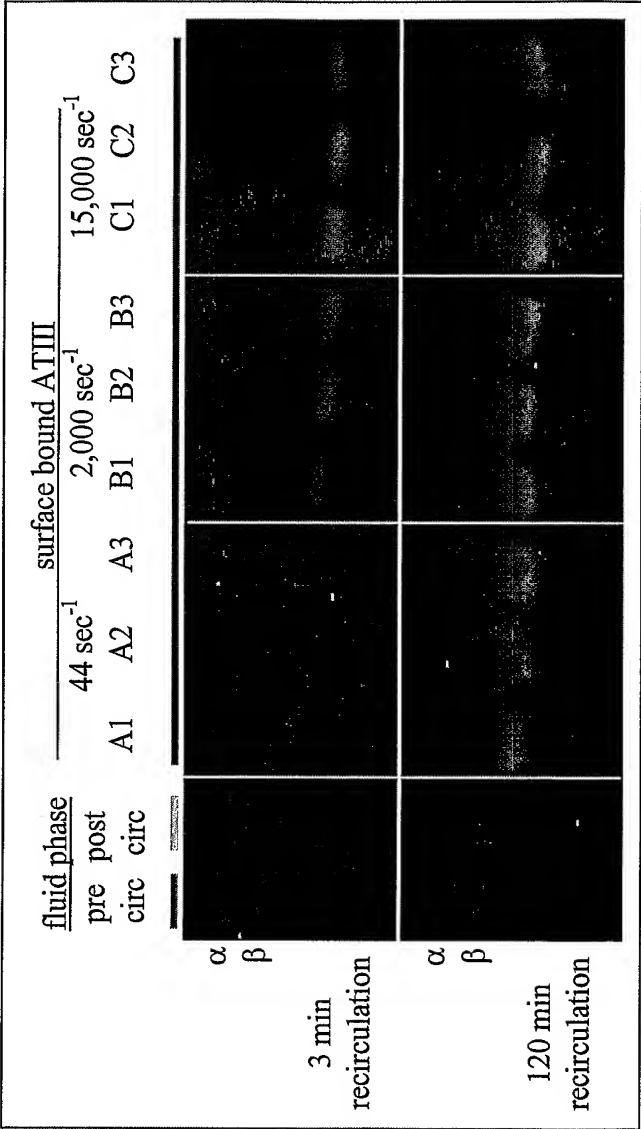


FIG. 9 Panel A

**A. WALL SHEAR RATE – DEPENDENT DIFFERENTIAL BINDING OF
ATIII ISOFORMS TO HEPARIN-COATED SURFACES**



10/17

Fig. 9 Panel B

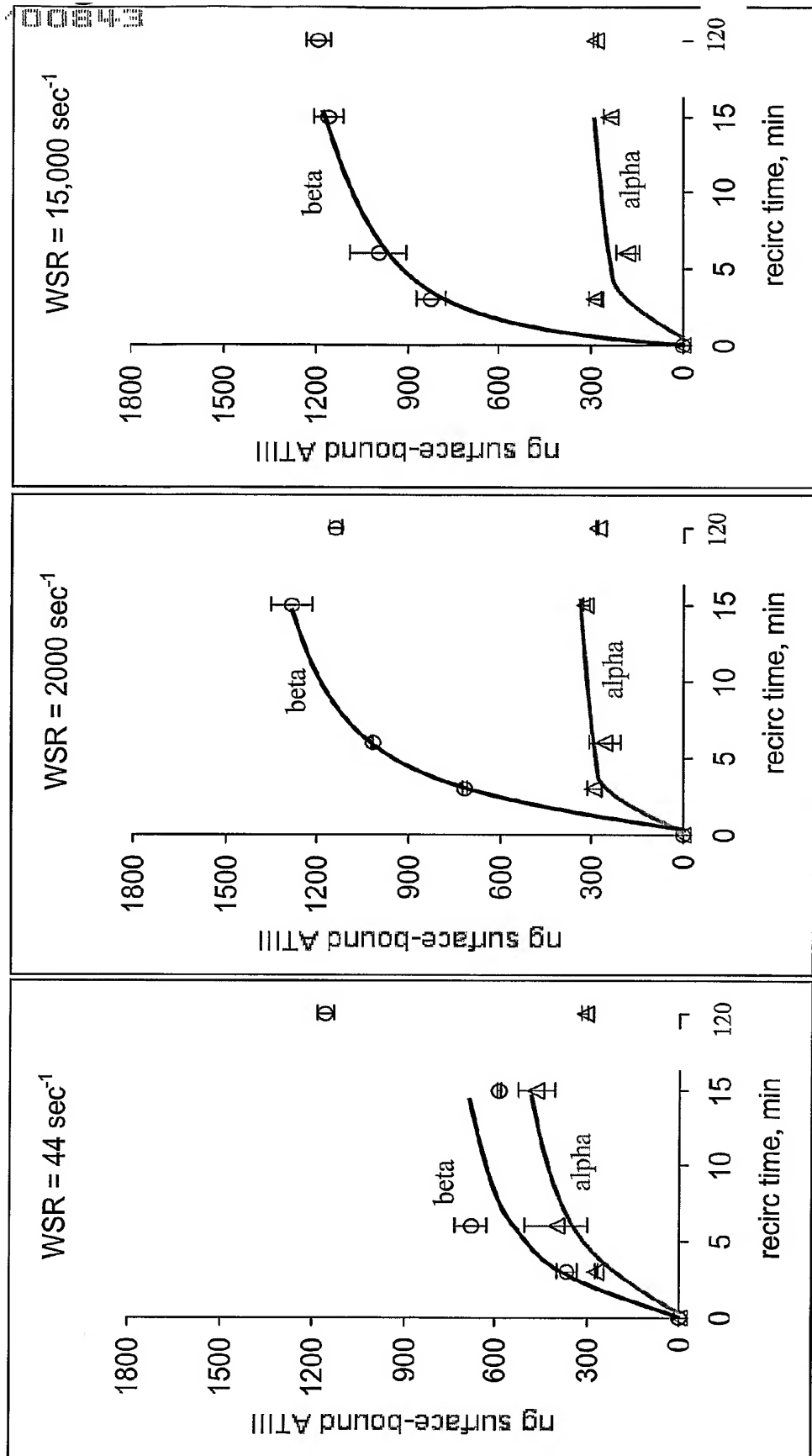


Fig. 9 Panel C

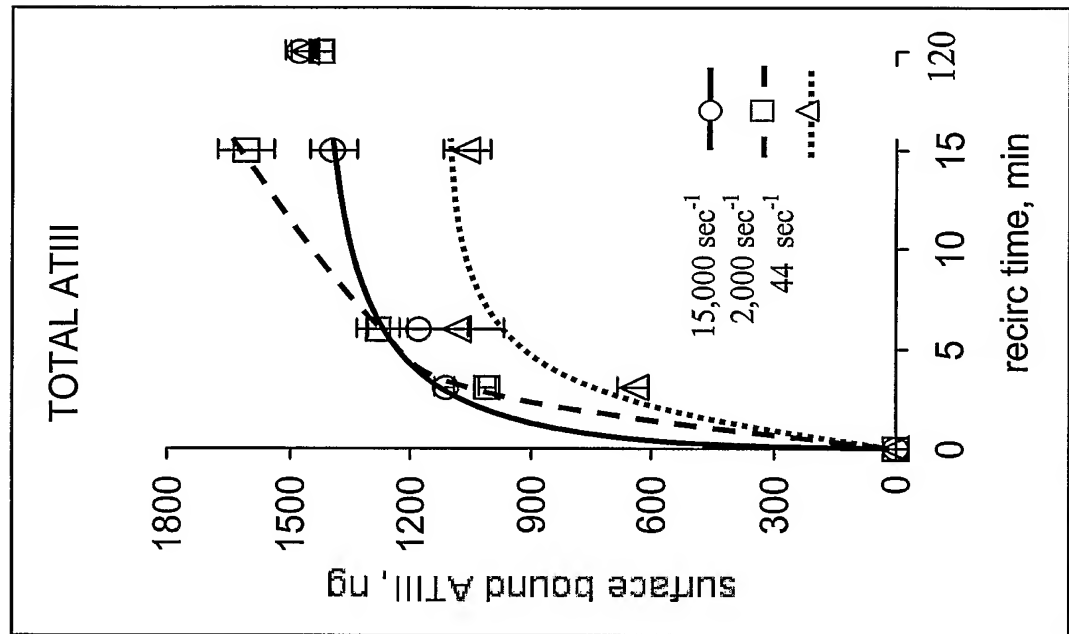


Fig. 10 Panel B

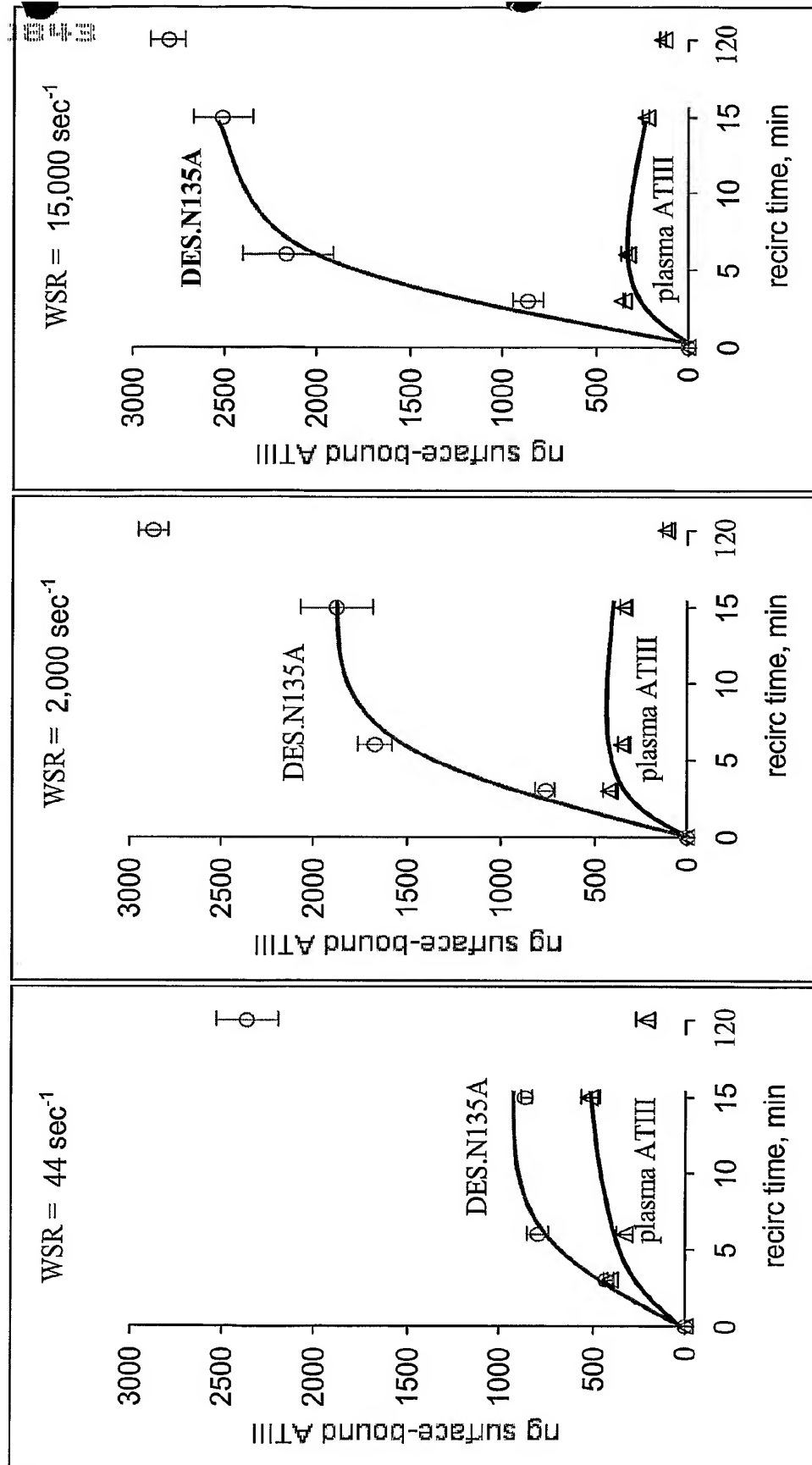


FIG. 11 Panel A

FUNCTIONAL INHIBITION OF FLOWING THROMBIN BY
SURFACE-TARGETED ATIIIS

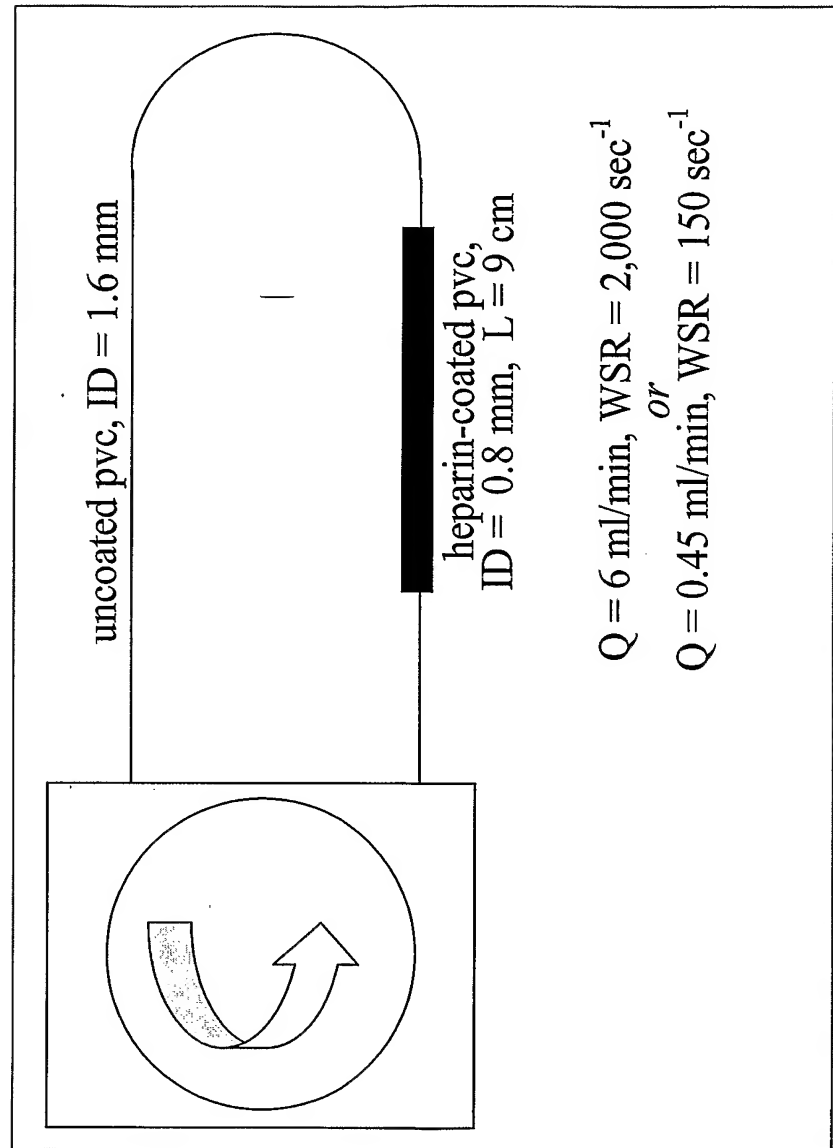


FIG. 11 Panel B

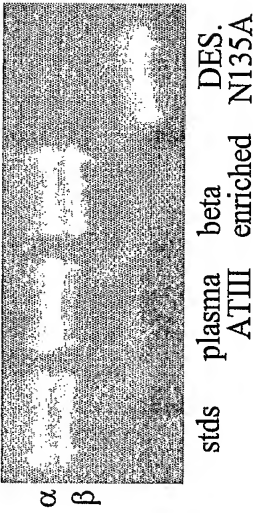
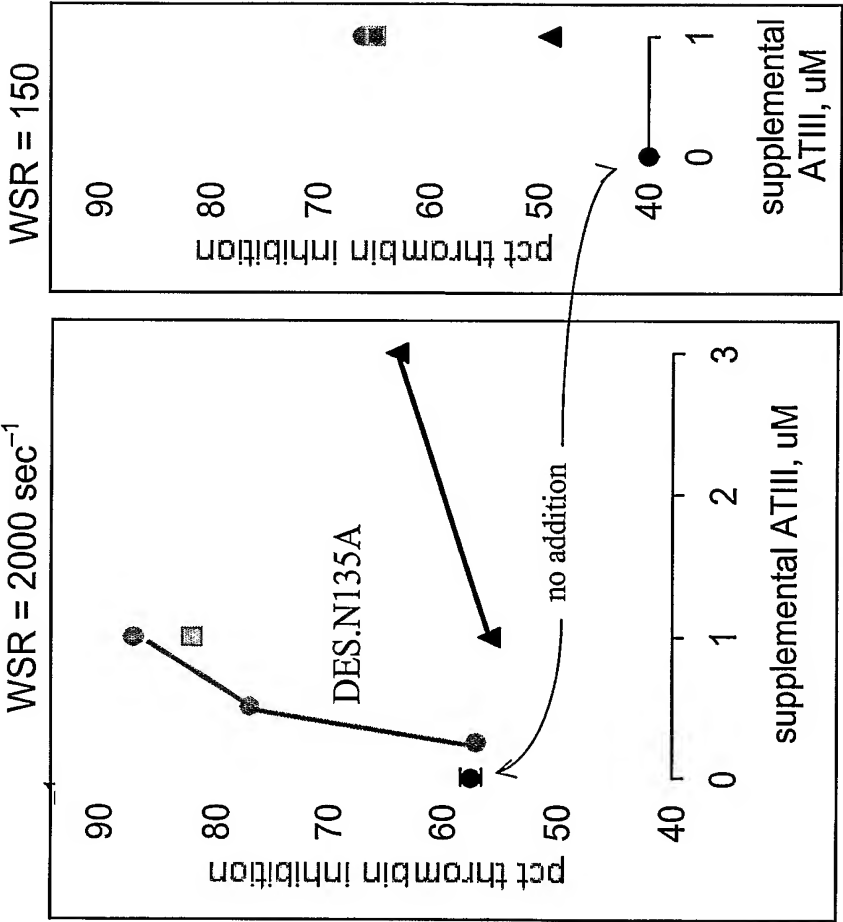
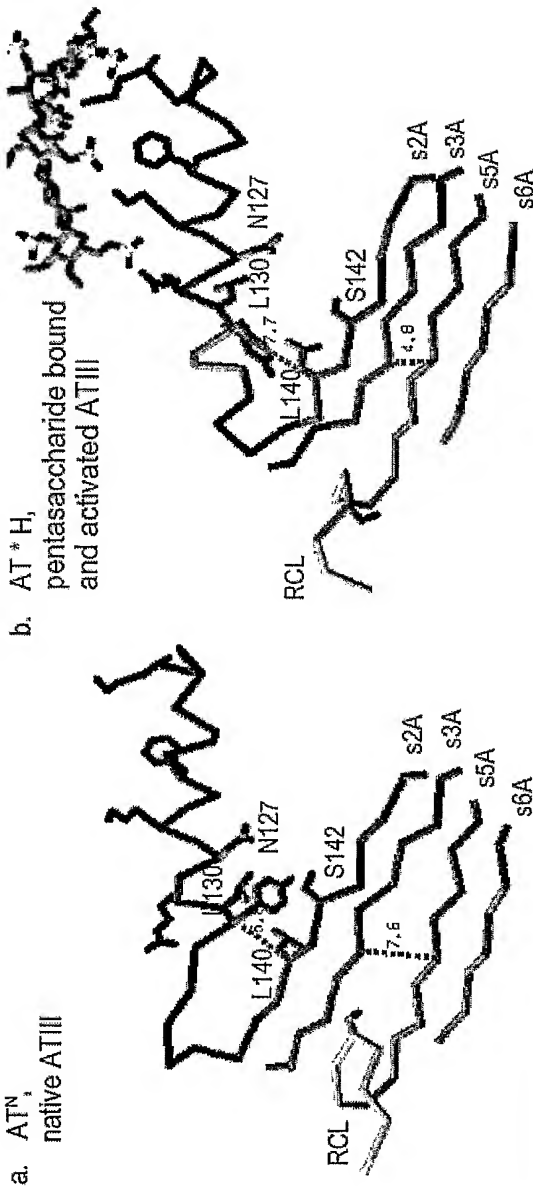


FIG. 12



c.

Tyrosine-131 distal ring carbon interactions with helix D and strand 2A residues in native and pentasaccharide-activated ATIII, Å					
		AT ^N (1E05i)		AT ^{*H} (1E03i)	
Y131	CE1	-	S142	CB	6.4
Y131	CE1	-	L140	CG	4.1
Y131	CE1	-	L130	CB	8.3
Y131	CZ	-	L130	CB	9.3
Y131	CZ	-	L130	CD1	11.3
Y131	CZ	-	S142	CB	6.9
Y131	CE2	-	L130	CB	9.1
Y131	CE2	-	L130	CD1	11.2
Y131	CE2	-	N127	CA	9.2
Y131	CE2	-	N127	CB	9.3
Y131	CE2	-	S142	CB	7.4

FIG. 13

